BIOMECHANICAL FACTORS FOR THE AETIOLOGY OF NAVICULAR DISEASE IN SPORTS HORSES

Franz K. Fuss, Angelika H. Fuss, Universität Wien, Wien, Austria

INTRODUCTION: Navicular disease is a common syndrome in sports horses such as gallopers, jumpers and western horses (especially quarter horses; Stashack, 1987). This syndrome causes forelimb lameness due to pain of the navicular bone (distal sesamoid of the horse digit, Figure 1), navicular bursitis and deep flexor tendon affection. When excellent horses develop navicular disease, they can no longer be used for contest purposes; however, for breeding purposes they are still desirable. Navicular disease is hereditary, but the mechanisms of heredity are, however, still unclear. Nevertheless, distinct morphological variations exist in the navicular bone which are also hereditary (Ueltschi et al., 1995). Our hypothesis on the transmission of navicular disease is that morphological variability causes differences in joint load and bone stress. The aim of this study was to analyze the loading situation of the navicular bone and the biomechanical effects of morphological variations of the navicular bone. The purpose of this study was to seek mechanically favorable and unfavorable parameters.

METHODS: In order to gather the data for the biomechanical analyses, we examined 87 German riding horses (between 3 and 5 years of age). Radiographs were taken of the latero-medial aspect of the forelimb phalanges. The horizontal X-ray beam was centered approximately 1cm above the coronary band in the midline. Radiographs lacking exact superposition of the medial and lateral contours of the distal part of phalanx II (coronary bone) were discarded. The animals showed neither signs of lameness nor of clinical or radiological affection of the forelimbs, and had neither anomalies in hoof shapes or the foot/pastern axis, nor prior illness, operations, or traumas. In 18 feet of warm-blood cadavers, we wove a metal filament (∅ 0.5 mm) into the DFT for diameter measurements. Then, radiographs were taken under tension of the DFT with a 50° toe position. In the radiographs, the rotation center (curvature center) of the coffin joint was determined. Based on this, we measured the lever arms (Fig. 1) of the acting forces considering the diameter of the DFT. The lever arm (p) of the proximal DFT force and the one(s) of the force of the joint between phalanx III (hoof bone) and the navicular bone were calculated relative to the lever arm (d = 1) of the distal DFT force. The measured angles are shown in Figure 1.

ANALYSIS: The free body diagram used in this analysis consists of the navicular bone and all forces acting on it. These are: (1) distal and (2) proximal force vectors of the DFT (PR), (3) the force of the joint between phalanx III and the navicular bone (SR), (4) the force of the joint between phalanx II and the navicular bone (JR, with its components Jx and Jy; coordinate system according to Fig. 1). The parameters sought are: (A) the force of the joint between phalanx III and the navicular bone in (SR in % of PR), (B) the force of the joint between phalanx II and the navicular bone in (JR in % of PR), (C) the inclination (angle φ) of the force of

the joint between phalanx II and the navicular bone (JR) to the y-axis, and (D) the joint surface stress (σ).

1) Moment (M) equilibrium:
The sum of all acting moments must be nil in any (rotation-) point. The curvature center of the articular surface was chosen as the rotation center, as the sought joint force (JR) passes through the curvature center (perpendicular to the joint surface tangent) and thus has a lever arm of size zero.

$$Mz: \quad d\,PR - p\,PR - s\,SR + JR \times 0 = 0 \qquad (1)$$

2) Force (F) equilibrium:

$$Fx: \quad -SR\sin(\tau) + PR\cos(\delta) - PR\cos(\pi) + Jx = 0 \qquad (2)$$

$$Fy: \quad SR\cos(\tau) - PR\sin(\delta) + PR\sin(\pi) + Jy = 0 \qquad (3)$$

(τ = phalanx III / navicular joint angle; δ, π = distal and proximal angle of the DFT; Fig. 1)

3) Calculation of the joint forces:
The equations (1)-(3) can now be transformed into the equations (4)-(6):

$$SR = (1-p)/s \qquad (4)$$

$$Jx = SR\sin(\tau) - \cos(\delta) + \cos(\pi) \qquad (5)$$

$$Jy = -SR\cos(\tau) + \sin(\delta) - \sin(\pi) \qquad (6)$$

$$JR = (Jx^2 + Jy^2)^{0.5} \qquad (7)$$

$$\varphi = \operatorname{atan}(Jx/Jy) \qquad (8)$$

The force vector JR intersects the joint surface at the pressure center.

4) Calculation of the cartilage pressure:
Compressive stress (σ) was calculated for joints of similar size (joint surface radius of the hoof joint r=1, medio-lateral extension of the navicular bone l=1) for reasons of comparability. ε and η are the angles proximal and distal of the joint force vector.

$$\varepsilon = -(\varphi - \beta) \qquad (9)$$

$$\eta = \gamma + \varepsilon \qquad (10)$$

These angles must be corrected for cases where the stress becomes negative (cases where the distance between the force vector and the middle of the proximo-distal extension [b] of the navicular bone is more than one sixth of b, according to the bending stress formulas for rectangular areas):

$$|\sin\varepsilon| < |\sin\eta|/2 \quad \rightarrow \quad |\sin\eta| = 2|\sin\varepsilon| \qquad (11)$$

$$|\sin\eta| < |\sin\varepsilon|/2 \quad \rightarrow \quad |\sin\varepsilon| = 2|\sin\eta| \qquad (12)$$

A negative stress (tensile stress) is of course not possible, as joint surfaces are not "glued" together.

$$b = r\sin\eta - r\sin\varepsilon \qquad (13)$$

$$h = b/2 - r\sin\eta \qquad (14)$$

κ = any angle between ε and η. The joint surface stress (σ) was calculated for the distal border ($\kappa = \varepsilon$), for the proximal border ($\kappa = \eta$), and for the position of the force vector (pressure center, $\kappa = 0$).

$$\sigma = ((JR\ h\ 12\ (\sin\kappa + h)) / (b^3\ l) + JR/(b\ l))\ (\cos\kappa)^2 \qquad (15)$$

This formula leads to the fact that the compressive stress vectors are perpendicular to the (cylindrical) joint surface and balanced relative to the pressure center.

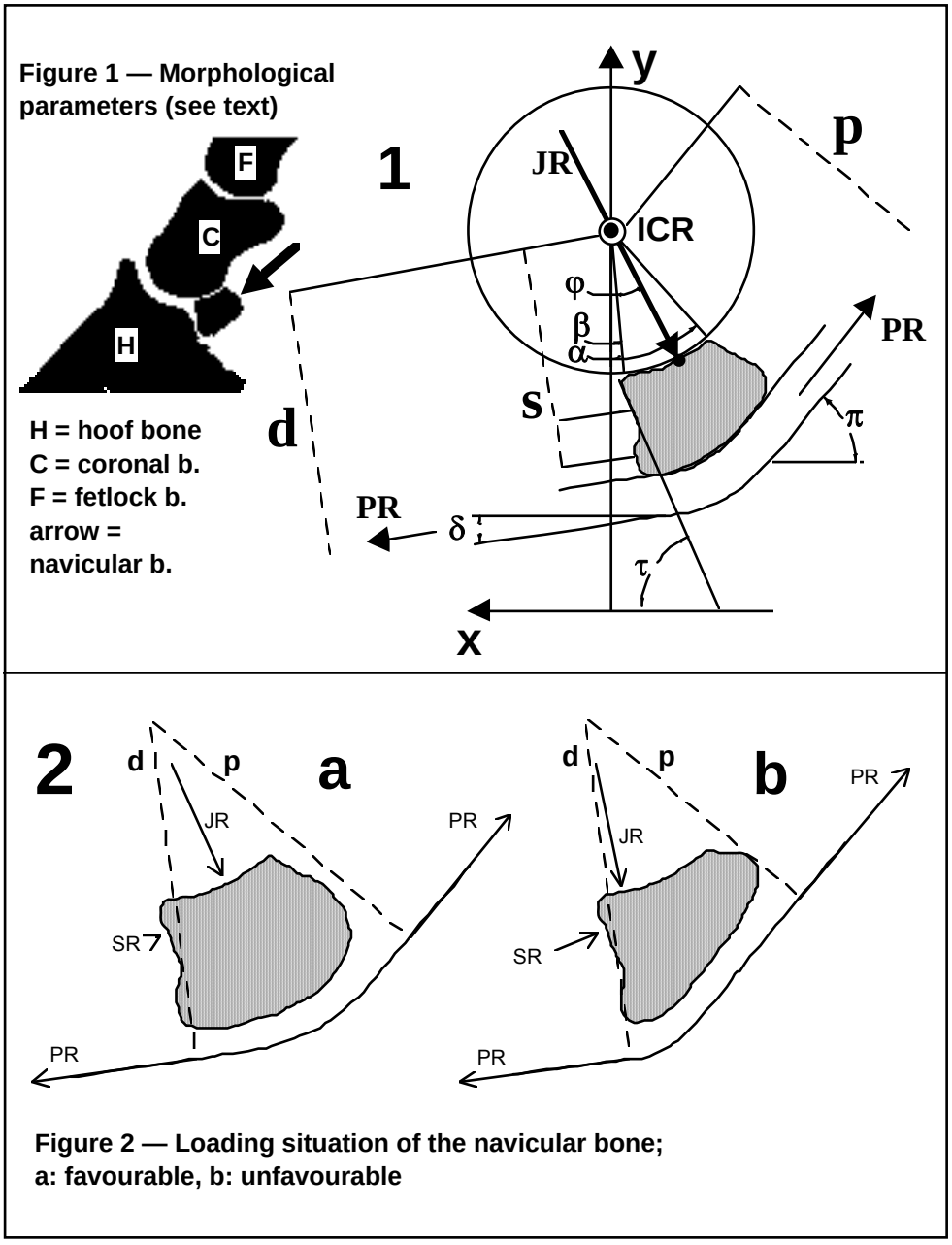

Figure 2 — Loading situation of the navicular bone; a: favourable, b: unfavourable

RESULTS: The lever arm (p) of the proximal DFT force is usually lower than that (d) of the distal DFT force, seldom higher. In navicular bones with a lever arm relation (p/d) of 0.8, the joint forces (JR, SR) are 33% higher than in lever arm relations of 1. Equally φ is 24° lower in lever arm relations of 0.8 than in lever arm relations of 1. An ideal stress situation occurs when both borders are equally stressed and maximal stress (σ=100%) appears in the middle of the joint surface

(Figure 2a). This is the case in lever arm relations of almost 1. In lever arm relations of 0.8 (Figure 2b), however, maximal stress appears at the distal border and is 3 times higher (σ=300%) than in ideal situations.
A favorable stress situation (Figure 2a) is given with a large proximal lever arm p: the force vector is positioned in the middle of the navicular bone and guarantees an optimal pressure distribution. An unfavorable stress situation (Figure 2b) is given in the case of a small proximal lever arm p: the force vector is situated at the distal border of the navicular bone and causes a distal overstress.
Three decisive (favorable / unfavorable) morphological factors can be distinguished: 1) large / small proximal lever (p) of the DFT (Figure 2), 2) distal / proximal position of the navicular bone (low / high α and β respectively), 3) large / small joint surface angle (γ). These three factors lead to a favorable / unfavorable loading situation (Figure 2): 1) small / high joint force vectors (JR and SR), 2) large / small angle φ of JR, 3) position of the force vector JR in the middle of the joint surface / at the distal border, 4) low / high surface stress (σ) at the distal border.

DISCUSSION: Unfavorable navicular mechanics will thus occur when the bone is overstressed in its distal border region. A comparison can be drawn here with navicular disease, where pathologic alterations also occur in the distal sector: the arterial supply shifts from distal to proximal with increasing navicular disease (Rijkenhuizen, 1990) and the foramina nutricia become canales sesamoidales. Colles (1979) explains the latter by a mere thrombosis progression, whilst other authors establish a mechanical relation: result of altering pressure and tension (Dämmrich et al., 1983), and expression of pressure atrophy (Scott 1968). It might be that distal overstress of the navicular bone causes vascular alteration. Further work, however, needs to be done to confirm such a hypothesis. A correlation between radiological morphology and clinical signs would be advantageous for conclusive proof; this, however, is probably not possible due to the multifactorial genesis of navicular disease.

CONCLUSIONS: A knowledge of morphologic variations and their biomechanical implications appears all the more important as breeding selection can prevent the hereditary transmission of unfavorable navicular morphology.

REFERENCES:

Colles, C. M. (1979). Ischaemic Necrosis of the Navicular Bone and its Treatment. *Veterinary Record* **104**, 133-137.

Dämmrich, K., Schebitz, H., Wintzer, H.-J. (1983). Die Podotrochlose des Pferdes aus heutiger Sicht. *Berliner Münchner Tierärztliche Wochenschrift* **96**, 293-302.

Rijkenhuizen, A. B. M. (1990). Die arterielle Blutgefäßversorgung des Strahlbeines und ihre Beziehung zur Podotrochlose. *Pferdeheilkunde* **6**, 253-260.

Scott, P. M. (1968). Bone Lesions in Pigmented Villonodular Synovitis. *Journal of Bone and Joint Surgery* **50B**, 306-311.

Stashak, T. S. (1987). Adams' Lameness in Horses (p. 499). 4th ed. Philadelphia: Lea & Febiger.

Ueltschi, G., Hornig, I., Stornetta, D. (1995). Beobachtungen zur Genetik der Podotrochlose. In P. F. Knezevic (Ed.), *Orthopädie bei Huf- und Klauentieren* (pp. 52-61). Stuttgart: Schattauer.